JOURNAL TEKNIK SIPIL DAN LINGKUNGAN| EISSN:2549-1407
https://journal.ipb.ac.id/index.php/jsil

Vol. 10 No. 02 October 2025
DOI: 10.29244/jsil.10.2.357-366

# Effects of Different Lateral Stiffeners to The Seismic Performance of 21-Storey Apartment Building Structure in Yogyakarta

**Ardityo Dwi Kuncoro* and Slamet Widodo**

Department of Civil Engineering and Planning Education, Engineering Faculty, Yogyakarta State University, Sleman, 55281
*Correspondences: ardityodwi.2021@student.uny.ac.id

**Abstract:** Rapid high-rise construction, especially in seismically active Java and Yogyakarta, demands lateral stiffness consistent with SDG 9 and SNI 1726:2019 to ensure resilience against earthquake actions. Shear walls and steel bracing are widely used to control interstory drift and stability, yet comparative evidence tailored to Yogyakarta remains limited. Methods used by using a finite-element model of a 21-story apartment and perform elastic response-spectrum analyses based on SNI 1726:2019. Four lateral systems are compared, emphasizing concentric X-bracing (CBF-X) and eccentric K-bracing (EBF-K). Performance metrics include interstory drift, P-Δ stability coefficients, and horizontal and vertical irregularities. Models incorporate rigid diaphragm assumptions, gravity and lateral load combinations, and cracked-section modifiers for shear walls consistent with code recommendations. Member forces were also checked. The results indicate that all structural configurations satisfy the standard requirements of SNI 1726-2019. The smallest interstory drift occurs in the structure with the K-bracing system, with minimum values in the X direction ranging from 3.992 mm and maximum 19.395 mm, and in the Y direction minimum from 1.172 mm and maximum 36.344 mm. The P–Delta effect shows the smallest stability coefficients in the K-bracing system, with X-direction minimum values of 0.0019 mm and maximum 0.0256 mm, and Y-direction minimum values of 0.0018 mm and maximum 0.0104 mm. Analysis of structural irregularities using X-ray diffraction yields superior results compared to other structures. For a tall building in Yogyakarta's seismic setting, combining shear walls with steel bracing is effective and code-compliant. Among the examined schemes, EBF-K minimizes drift and P-Δ effects, offering superior lateral stiffness and energy dissipation, whereas CBF-X excels in meeting irregularity criteria and maintaining global stability. The results provide location-specific guidance for selecting lateral systems in Indonesian high-rise design and support performance-oriented detailing under SNI 1726:2019.

**Keywords:** Tall Building, Steel Brace, Shear Wall, Lateral Stiffness, Spectrum Response

**Submitted**: 26 Sep 2025
**Revised:** 07 Oct 2025
**Accepted**: 25 Oct 2025

## 1. Introduction

The construction of tall buildings with ever-increasing heights has been happening on a massive scale over the past 20 years. Thousands of high-rise buildings and hundreds of super high-rise buildings have been constructed in cities around the world. This is due to various factors, such as population growth, massive globalization, drastic urban transformation, and land constraints [1]. Aligned with Sustainable Development Goal (SDG) 9, the pursuit of resilient, sustainable, and reliable infrastructure development constitutes a key effort to foster economic growth and enhance human well-being [2]. Resilient infrastructure refers to the capacity of structural systems to maintain their stiffness. Resilient infrastructure refers to the ability of structural systems to preserve their stiffness. Adequate stiffness is particularly crucial in high-rise buildings to withstand lateral forces induced by earthquakes [3].

The presence of earthquake hazards poses significant challenges for seismic design in terms of stiffness, strength, and stability, particularly in regions with high seismicity.

Indonesia is located in one of the most seismically active regions of the world and has experienced many major earthquakes in the past [4]. Java, which is often the center of major earthquake activity, is the fourth largest island with the highest population density in Indonesia. Java is part of a complex convergence zone between the Eurasian plate and the Indo-Australian plate [5] [6]. Large earthquakes close to the Java trough are usually inter-plate fault events along the plate between the Australian and Sunda plates; these earthquakes generally have a high tsunami potential due to their shallow depth [7]. The region along the southern coast of Java has only experienced sizable earthquakes over the past 100 years. However, recent research on tsunami deposits along the south coast of Java suggests that megathrust events do occur in this region and have a return period of 500 years [8].

The Special Region of Yogyakarta is located near the collision zone in southern Java, making it prone to tectonic activity. This is evident from several earthquakes in recent years. One of the largest was the 2006 Yogyakarta earthquake, which caused significant damage, both material and human casualties. The tremors destroyed many buildings, although the level of damage varied from area to area [9]. The earthquake was thought to have been caused by the movement of an active fault east of Yogyakarta, namely the Opak Fault, with a north-south shift. The Opak Fault could become active again at any time, so disaster mitigation is needed in the design of buildings to reduce damage and casualties in the future [10]. Areas with a high risk of earthquakes, such as Yogyakarta, require structural planning that is specifically designed to withstand seismic loads [11]. Therefore, buildings must be designed with structural principles that can accommodate lateral forces, thereby minimizing the risk of damage during an earthquake.

Therefore, to withstand lateral loads, especially those caused by earthquakes, it is necessary to increase the stiffness of the structure or the ability of the building to withstand lateral loads. Adequate stiffness is very important in high-rise buildings to withstand lateral pressures caused by earthquakes. To increase structural stiffness in reducing earthquake loads, shear walls and steel braces are used as part of the building. This can be used to improve the seismic response of the structure. The main concern in structural design is the safety of the structure during a major earthquake, so it is very important to ensure adequate lateral stiffness to withstand earthquake loads [12].

Shear walls are vertical structural components used to reinforce buildings against lateral forces such as earthquakes [13]. These structures are characterized by high rigidity and strength, enabling them to withstand large lateral loads while supporting the gravitational load of the building. Thus, shear walls effectively reduce the effects of shocks that cause horizontal shifts in structures, thereby minimizing the risk of damage to buildings and objects inside them [14]. In addition, shear walls are essential in maintaining floor stability to prevent collapse when buildings experience lateral shocks due to earthquake activity. Therefore, the application of shear walls in structural planning is the main solution in efforts to mitigate the risk of damage caused by earthquakes [15].

In addition to using sliding walls, efforts to increase the resistance of building structures to lateral forces can also be made by applying steel bracing frames. Bracing frames are diagonal steel structural systems that function to reduce deflection and lateral movement caused by external forces such as earthquakes and wind gusts [16]. This system is considered effective, especially in seismic retrofitting, because it has a high level of rigidity that can significantly reduce lateral displacement and bending moments acting on columns [17].

## 2. Methods

### *2.1. Materials*

The study site is a 21–story apartment building in Palagan Tentara Pelajar Street, Ngaglik, Sleman, Yogyakarta as shown in **Figure 1**, selected as a representative case to evaluate and optimize lateral force–resisting systems—specifically shear walls and steel bracing. This location is relevant because the seismic conditions in Yogyakarta are prone to earthquakes, so structural strengthening of tall buildings is needed to ensure their safety and stability. A numerical finite-element modeling approach is employed to simulate seismic response and mechanical behavior, thereby assessing the effectiveness of alternative lateral systems for high-rise buildings.

Design inputs comprise building specifications, material properties, structural data, and architectural information curated to meet safety, functional, and aesthetic requirements. The prototype building has a total height of 61.5 m with variable story elevations and serves primarily as a residential apartment complex. The structural system adopts a Special Moment Resisting Frame (SMRF; Indonesian: SRPMK) with shear walls, proportioned to resist earthquake-induced lateral actions in accordance with SNI 1726:2019.

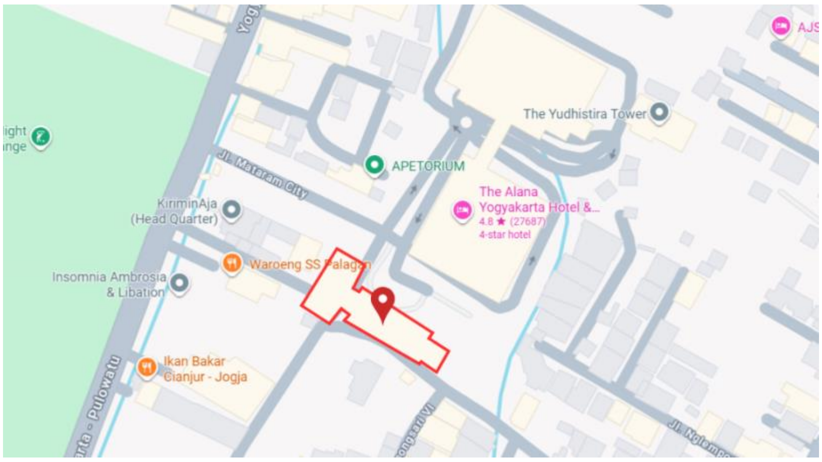


**Figure 1**. Research Location

### *2.2. Research Procedures*

The stages of analysis in this study were carried out systematically through several main interrelated steps as shown in **Figure 2**, these stages involved:

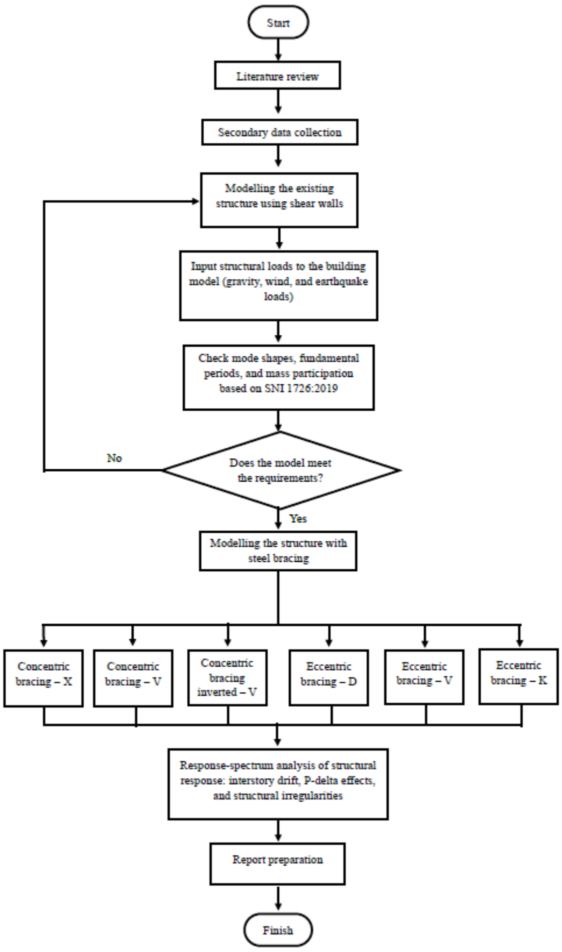


**Figure 2**. Flowchart procedure

The analysis proceeded systematically through interrelated stages as illustrated in **Figure 2**. First, a literature review was undertaken to consolidate the theoretical and empirical foundation for lateral-force–resisting systems in high-rise buildings aimed at improving seismic performance. The review encompassed SNI structural design standards, local and international journal articles, prior studies on shear walls and steel bracing, and authoritative textbooks, thereby establishing the state of the art and identifying methodological benchmarks for this study.

Next, secondary data were compiled to support building design assumptions and subsequent structural analysis. The dataset—obtained from the contractor of a 21-story apartment building in Yogyakarta—included architectural floor plans, total elevations, and dimensions of key structural components such as slabs, beams, columns, and shear walls. These materials provided the geometric and material inputs for model development.

Using these inputs, a finite-element structural model was developed to represent the baseline building configuration. The baseline adopts reinforced-concrete shear walls as the primary lateral-force–resisting system, located at the lift core and at building corners, with a uniform wall thickness of 400 mm consistent with design practice for high-rise structures. The initial three-dimensional representation of the building is presented in **Figure 3**.

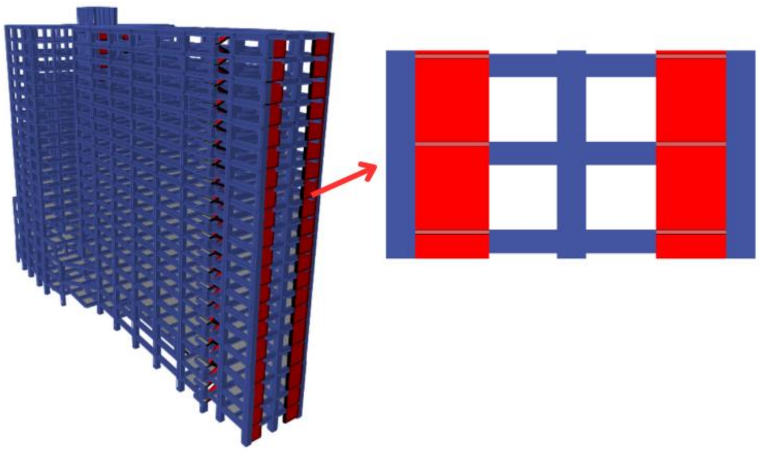

**Figure 3**. Existing model with shear walls

Design actions were then applied to the model in accordance with SNI 1727:2020, including superimposed dead loads, live loads, earthquake loads, wind loads, and roof rain loads. Load magnitudes and combinations were assigned to reflect realistic service conditions over the building's life and to ensure that safety and reliability criteria were addressed within a code-compliant framework.

To verify dynamic characteristics, mode shapes, fundamental periods, and mass participation were evaluated against SNI 1726:2019. The fundamental period estimates were used to characterize primary vibration behavior, while the mode shapes provided insight into story-wise deformation patterns. The number of modes included in the analysis was increased iteratively until the cumulative mass participation in both principal directions (X and Y) reached at least 90%, satisfying SNI 1726:2019 requirements for reliable dynamic response calculations.

Alternative lateral systems employing steel bracing were then configured as substitutes for the baseline shear walls. Two scheme families were considered: concentric braced frames (CBF) and eccentric braced frames (EBF). The CBF schemes were selected to leverage increased lateral stiffness with comparatively lower structural weight, employing X-, V-, and inverted-V bracing around the building perimeter as shown in **Figure 4**.

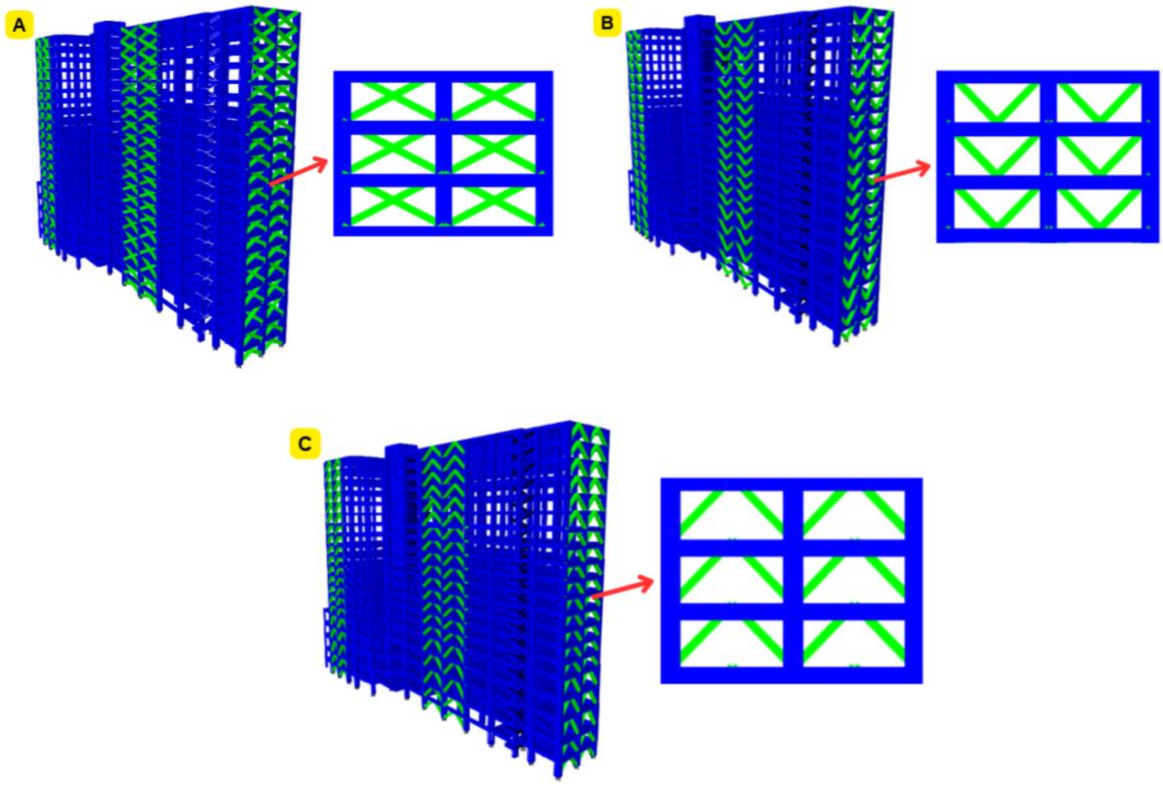


**Figure 4**. Concentric bracing model. Type X model (A); Type V model (B); Type V-inverted model (C)

EBF schemes enhance seismic resilience by dissipating energy through link deformation. Perimeter D-, V-, and K-type layouts channel lateral forces while reducing stiffness versus CBFs. Short links yield in shear; longer links in flexure, with capacity design protecting adjacent members. Inelasticity is confined to replaceable links, improving drift capacity, flexibility, and repairability, and enabling stable hysteresis and rapid post-earthquake recovery, as shown **Figure 5**.

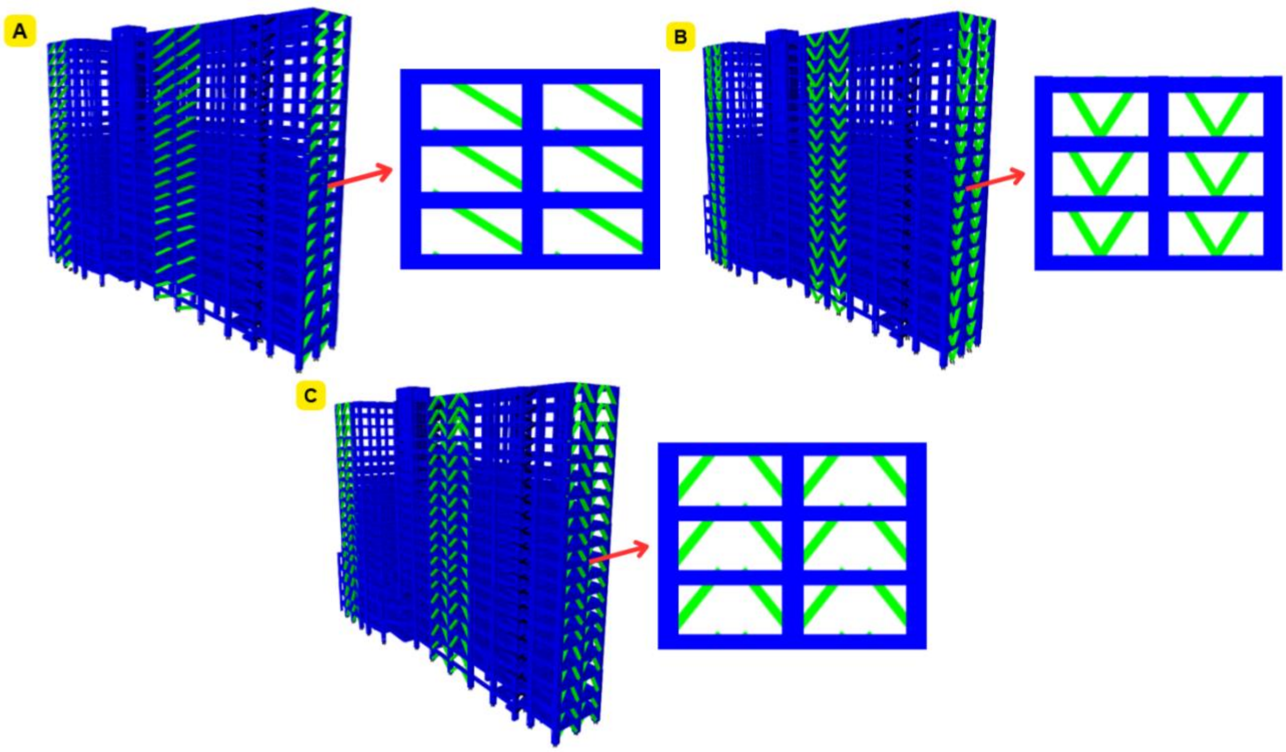


**Figure 5**. Eccentric bracing model. Type D model (A); Type V model (B); Type K model (C)

Finally, response-spectrum analysis was performed to quantify seismic demands and assess structural performance across all configurations. The evaluation included checks on interstory drift, P–Δ effects, and plan and vertical irregularities, ensuring that each model met codified performance targets and enabling a comparative appraisal of the alternative lateral-resisting strategies.

### *2.3. Material Specification*

In this building design, the material specifications comprise concrete, reinforcing steel, and steel bracing elements. Concrete is used as the primary material for vertical members such as columns and shear walls, as well as horizontal members such as beams and slabs. Reinforcing steel is provided to strengthen the concrete so it can resist tensile and shear forces. Meanwhile, steel bracing serves as the lateral force–resisting system designed to increase stiffness and stability against lateral actions such as earthquakes.

1. Concrete

   The concrete used in this study is selected in accordance with design standards to ensure strength, durability, and seismic resistance. Specifications include compressive strength, modulus of elasticity, and Poisson's ratio, which govern the structural response to loads. Full details are presented in the following **Table 1**.

**Table 1**. Concrete material specification

| Aspect | Value |
| --- | --- |
| Compressive strength of concrete, $f'_c$ | 30 MPa |
| Modulus of elasticity of concrete, $E_c$ | 25,742.96 MPa |
| Poisson's ratio of concrete, $v$ | 0.2 |
| Density of concrete | 2,400 kg/m$^3$ |
| Function | Columns, slabs, beams, shear walls |

2. Steel

   The steel material is selected to provide strength, ductility, and resistance to gravity and seismic loads. It contributes to stiffness, stability, and energy dissipation while maintaining structural integrity in line with design provisions. Full details are presented in the following **Table 2**.

**Table 2**. Steel reinforcement material specifications

| Aspect | Value |
| --- | --- |
| Yield strength of longitudinal reinforcement, BjTS 420B ($f_y$) | 420 MPa |
| Tensile (ultimate) strength of longitudinal reinforcement, BjTS 420B ($f_u$) | 525 MPa |
| Yield strength of transverse reinforcement, BjTS 280 ($f_y$) | 280 MPa |
| Tensile (ultimate) strength of transverse reinforcement, BjTS 280 ($f_u$) | 350 MPa |
| Modulus of elasticity of steel, $E_s$ | 200000 MPa |
| Poisson's ratio of steel, $v$ | 0.3 |

3. Steel Bracing

   Steel bracing increases lateral stiffness, reduces drift, and enhances seismic performance. These members transfer horizontal forces to vertical elements, minimize structural deformation, and maximize energy dissipation during earthquakes. Full details are presented in the following **Table 3**.

**Table 3**. Steel bracing material specifications

| Aspect | Value |
|---|---|
| Steel grade | BJ 41 |
| Yield strength, $F_y$ | 250 MPa |
| Ultimate tensile strength, $F_u$ | 410 MPa |
| Poisson's ratio, $v$ | 0.3 |
| Density | 4,850 kg/m$^3$ |

## 3. Result and Discussion

Through trial-and-error testing of various bracing configurations, including X, V, and inverted-V types for concentric bracing, and D, V, and K types for eccentric bracing, the combination of a concentric X-brace and an eccentric K-brace delivered the optimal structural performance. This study presents a comprehensive comparative evaluation of four different lateral stiffening systems in a 21-story apartment building in Yogyakarta: a bare open frame (no stiffeners); a shear wall system; a concentric X-braced frame (CBF-X); and an eccentric K-braced frame (EBF-K).

This direct side-by-side comparison of multiple lateral systems within a single building model is novel in Indonesian high-rise design, as previous studies in Yogyakarta have not directly compared such a range of systems in one structure. All the examined configurations meet the seismic performance requirements of SNI 1726:2019 (including interstory drift, P-delta effect, and irregularity structures), indicating that each system can provide at least a minimally acceptable level of seismic resistance. However, the detailed results reveal significant differences in relative performance, highlighting that the choice of lateral system is crucial for performance-based design under local seismic conditions.

### *3.1. Interstory Drift*

Interstory drift demands were calculated for each model in both principal directions and evaluated against the limit of 0.02 times the story height (0.02*h) prescribed by SNI 1726:2019. All schemes remained within this allowable drift, but the magnitudes varied considerably. Detailed interstory-drift results for the four structural models are shown in **Figure 6** and **7**.

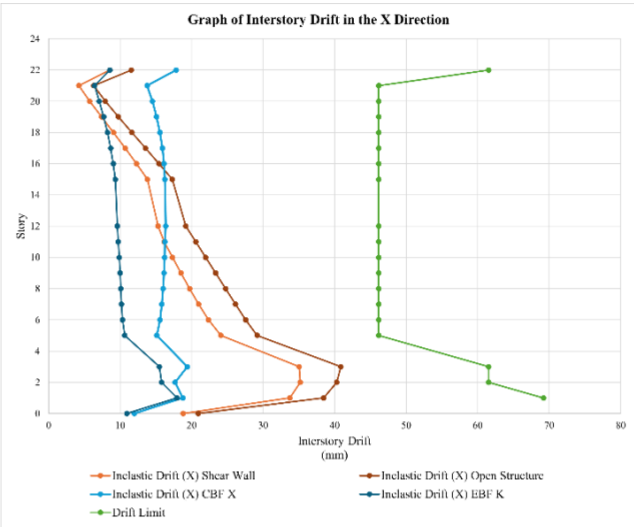


**Figure 6**. Graph of Interstory Drift in The X Direction

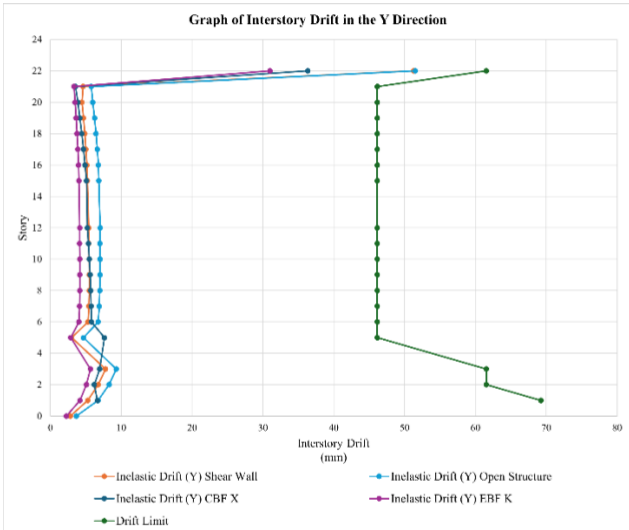


**Figure7**. Graph of Interstory Drift in The Y Direction

The eccentric K-bracing (EBF-K) system achieved the greatest reduction in lateral deflections among the four systems (**Table 4**). It exhibited the smallest interstory drifts, with maximum story drift on the order of 17.948 mm in the X-direction and 31.008 mm in the Y-direction. In contrast, the open frame (unbraced) structure experienced the largest drifts (significantly higher than those of the braced or shear-wall models), while the shear wall and X-braced (CBF-X) models showed intermediate performance.

These results clearly indicate that adding K-type eccentric steel bracing markedly improves lateral stiffness and drift control. The K-braced structure's drifts are substantially lower than the unbraced frame and modestly lower than even the shear wall or X-braced cases, demonstrating superior ability to limit earthquake-induced story displacements. In summary, the EBF-K system proved most effective in controlling interstory drift demands, which is a critical factor for preventing non-structural damage and maintaining building functionality after seismic events.

**Table 4**. Maximum story drift of four different lateral stiffening systems

| Structural Types | Maximum Interstory Drift X Direction (mm) | Maximum Interstory Drift Y Direction (mm) |
|---|---|---|
| Open frame | 40.854 | 51.515 |
| Shear wall system | 35.189 | 51.266 |
| Concentric X-braced frame | 19.395 | 36.344 |
| Eccentric K-braced frame | 17.948 | 31.008 |

*3.2. P-Delta Effect*

The second-order P–Δ effects (stability index due to gravity load acting on displaced structure) were evaluated via stability coefficients for each configuration. All models showed stability coefficient values well below critical thresholds (e.g., significantly under 0.1, indicating P-Δ effects are within stable limits). The calculated P–Δ responses for the four structural models are presented in **Figure 8** and **9**.

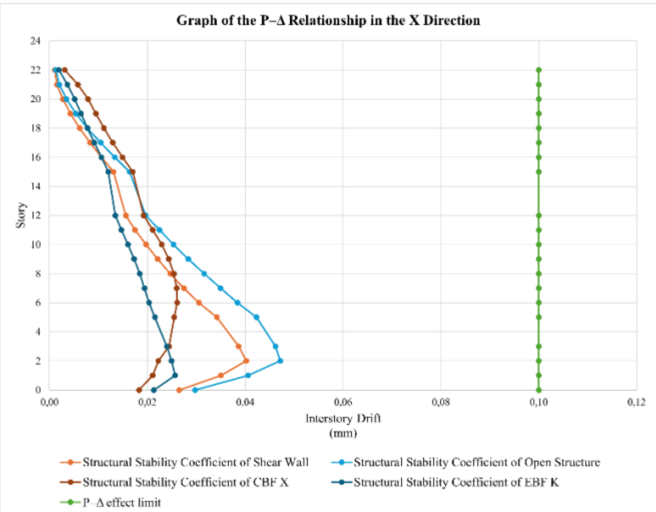


**Figure 8.** Graph of The P-Delta Relationship in The X Direction

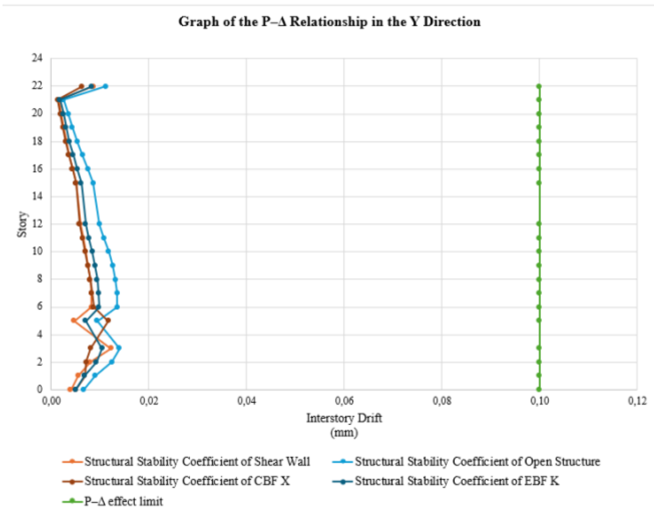


**Figure 9**. Graph of The P-Delta Relationship in The Y Direction

Consistent with the drift trends, the EBF-K braced frame had the smallest P–Δ stability coefficients of all systems (**Table 5**). In the K-braced structure, the maximum stability index in the X-direction was approximately 0.0256 (dimensionless), and in the Y-direction about 0.0104, markedly lower than the corresponding values in the other three models. These low stability indices for EBF-K reflect its enhanced lateral stiffness and energy dissipation capacity, which effectively mitigate second-order amplification of displacements. The open frame exhibited the highest stability coefficients (indicating the most pronounced P-Δ effects, though still within acceptable range), whereas the shear wall and CBF-X frames fell in between. The significantly reduced P-Δ demand in the K-braced system further underscores its advantage in maintaining global stability under seismic loading. By minimizing gravity-driven incremental deflections, the EBF-K scheme ensures that the structure remains well within the stable regime during strong earthquakes, thereby improving overall seismic reliability deflections, the EBF-K scheme ensures that the structure remains well within the stable regime during strong earthquakes, thereby improving overall seismic reliability.

Table 5. Maximum P-Δ effect of four different lateral stiffening systems

| Structural Types | Maximum P-Δ Effect X Direction | Maximum P-Δ Effect Y Direction |
|---|---|---|
| Open frame | 0.0472 | 0.0140 |
| Shear wall system | 0.0402 | 0.0123 |
| Concentric X-braced frame | 0.0261 | 0.0118 |
| Eccentric K-braced frame | 0.0256 | 0.0104 |

*3.3. Irregularity Analysis*

Structural irregularity checks showed that all systems met code requirements without significant soft-story or torsional issues (**Table 6**). The concentric X-braced frame (CBF-X) achieved the most uniform stiffness and deformation, minimizing torsional effects through its symmetric layout. The eccentric K-braced frame (EBF-K) reduced overall drift but introduced slight stiffness asymmetry, making its torsional response marginally less favorable though still within limits. The shear wall and bare frame systems also satisfied regularity criteria but were less uniform. Overall, CBF-X provided the most balanced lateral behavior, highlighting that well-distributed stiffness is crucial for maintaining seismic regularity and avoiding localized damage.

Table 6. Horizontal torsion irregularities result

| Storey | Open Frame | | Shear Wall System | | CBF-X | | EBF-K | |
|---|---|---|---|---|---|---|---|---|
| | X-Dir | Y-Dir | X-Dir | Y-Dir | X-Dir | Y-Dir | X-Dir | Y-Dir |
| | $\Delta_{max}/\Delta_{avg}$ | | | | | | | |
| Top | 1.945 | 1.895 | 1.954 | 1.898 | 1.888 | 1.893 | 1.917 | 1.896 |
| Rooftop | 2 | 2 | 2 | 2 | 2 | 2 | 2 | 2 |
| 20 | 2 | 2 | 2 | 2 | 2 | 2 | 2 | 2 |
| 19 | 2 | 2 | 2 | 2 | 2 | 2 | 2 | 2 |
| 18 | 2 | 2 | 2 | 2 | 2 | 2 | 2 | 2 |
| 17 | 2 | 2 | 2 | 2 | 2 | 2 | 2 | 2 |
| 16 | 2 | 2 | 2 | 2 | 2 | 2 | 2 | 2 |
| 15 | 2 | 2 | 2 | 2 | 2 | 2 | 2 | 2 |
| 12 | 2 | 2 | 2 | 2 | 2 | 2 | 2 | 2 |
| 11 | 2 | 2 | 2 | 2 | 2 | 2 | 2 | 2 |
| 10 | 2 | 2 | 2 | 2 | 2 | 2 | 2 | 2 |
| 9 | 2 | 2 | 2 | 2 | 2 | 2 | 2 | 2 |
| 8 | 2 | 2 | 2 | 2 | 2 | 2 | 2 | 2 |
| 7 | 2 | 2 | 2 | 2 | 2 | 2 | 2 | 2 |
| 6 | 2 | 2 | 2 | 2 | 2 | 2 | 2 | 2 |
| 5 | 2 | 2 | 2 | 2 | 2 | 2 | 2 | 2 |
| 3 | 1.048 | 1.352 | 1.04 | 1.349 | 1.151 | 1.417 | 1.108 | 1.361 |
| 2 | 1.671 | 1.417 | 1.579 | 1.336 | 1.152 | 1.416 | 1.37 | 1.33 |
| 1 | 1.06 | 1.473 | 1.039 | 1.326 | 1.146 | 1.399 | 1.09 | 1.3 |
| Lobby | 1.064 | 1.531 | 1.042 | 1.32 | 1.115 | 1.347 | 1.153 | 1.309 |
| Basement | 1.077 | 1.52 | 1.066 | 1.344 | 1.182 | 1.378 | 1.155 | 1.369 |

## 4. Conclusion

Based on numerical analyses of interstory drift, P–Δ effects, and structural irregularities, this study finds that the eccentric K-bracing system is the most effective configuration for enhancing the seismic performance of high-rise buildings. It delivers the smallest interstory drifts in both principal directions (X and Y) and P–Δ stability coefficients well below the $\theta \leq 0.10$ limit specified by SNI 1726:2019, indicating optimal lateral deformation capacity and global stability. Meanwhile, the concentric X-bracing system excels at controlling irregularities, particularly by avoiding torsional irregularity. Accordingly, a strategic combination of eccentric and concentric bracing can offer an effective earthquake-resistant design solution, especially in high-seismic regions such as Yogyakarta.

Practitioners are encouraged to implement eccentric K-bracing in high-rise buildings to control lateral deformations and enhance energy dissipation, while employing concentric X-bracing to address structural irregularities. Future research may investigate nonlinear behavior and energy-dissipation capacity through experimental programs or advanced simulations.

## References


[1] K. Al-Kodmany, Q. (Charlie) Xue, and C. Sun, "Reconfiguring Vertical Urbanism: The Example of Tall Buildings and Transit-Oriented Development (TB-TOD) in Hong Kong," *Buildings*, vol. 12, no. 2, p. 197, Feb. 2022, doi: 10.3390/buildings12020197.

[2] "THE 17 GOALS | Sustainable Development." Accessed: Sep. 26, 2025. [Online]. Available: https://sdgs.un.org/goals

[3] L. Velasco, A. Hospitaler, and H. Guerrero, "Optimal design of the seismic retrofitting of reinforced concrete framed structures using BRBs," *Bull. Earthq. Eng.*, vol. 20, no. 10, pp. 5135–5160, Aug. 2022, doi: 10.1007/s10518-022-01394-z.

[4] M. Irsyam *et al.*, "Development of the 2017 national seismic hazard maps of Indonesia," *Earthq. Spectra*, vol. 36, no. 1_suppl, pp. 112–136, Oct. 2020, doi: 10.1177/8755293020951206.

[5] H. U. Schlüter *et al.*, "Tectonic features of the southern Sumatra-western Java forearc of Indonesia," *Tectonics*, vol. 21, no. 5, Oct. 2002, doi: 10.1029/2001TC901048.

[6] I. Metcalfe, "Tectonic framework and Phanerozoic evolution of Sundaland," *Gondwana Res.*, vol. 19, no. 1, pp. 3–21, Jan. 2011, doi: 10.1016/j.gr.2010.02.016.

[7] E. S. Jones *et al.*, "Seismicity of the Earth 1900-2012 Java and vicinity," U.S. Geological Survey, 2010-1083-N, 2014. doi: 10.3133/ofr20101083N.

[8] R. Harris *et al.*, "Seismic and tsunami risk of the Java Trench and implementation of risk reduction strategies," in *SEG Technical Program Expanded Abstracts 2019*, San Antonio, Texas: Society of Exploration Geophysicists, Aug. 2019, pp. 4786–4789. doi: 10.1190/segam2019-3215203.1.

[9] E. Cahyani, W. N. Afrita, A. E. N. Aza, and D. R. S. Sumunar, "Pengembangan sistem jaringan evakuasi bencana likuifaksi di wilayah Sesar Opak," *Geomedia Maj. Ilm. Dan Inf. Kegeografian*, vol. 17, no. 1, Nov. 2019, doi: 10.21831/gm.v17i1.28297.

[10] M. T. Aurora, A. N. Islamiyat, W. B. Santosa, and B. Kusumahasto, "Morphotectonic Analysis of Opak Fault as an Application for Desaster Mitigation of Yogyakarta Earthquake," 2022.

[11] A. Shamil and D. J. Dhyani, "'COMPARATIVE SEISMIC EVALUATION OF RESPONSE OF RC BUILDING WITH SHEAR WALL FRAME AND DIFFERENT BRACING SYSTEMS,'" *Int. Res. J. Eng. Technol. IRJET*, vol. 05, no. 04, pp. 917–921, Apr. 2018.

[12] K. Vijetha and D. B. P. Rao, "Comparative Study of Shear Walls and Bracings for A Multistoried Structure Under Seismic Loading," *Int. J. Eng. Res. Technol.*, vol. 8, no. 7, Jul. 2019, doi: 10.17577/IJERTV8IS070174.

[13] J. Tarigan, J. Manggala, and T. Sitorus, "The effect of shear wall location in resisting earthquake," *IOP Conf. Ser. Mater. Sci. Eng.*, vol. 309, p. 012077, Feb. 2018, doi: 10.1088/1757-899X/309/1/012077.

[14] M. Tumpu, H. Parung, M. W. Tjaronge, and A. Amiruddin, "(PDF) Kinerja Pembebanan Lateral Dinding Geser Beton Ringan," ResearchGate. Accessed: Sep. 26, 2025. [Online]. Available: https://www.researchgate.net/publication/356789589_Kinerja_Pembebanan_Lateral_Dinding_Geser_Beton_Ringan

[15] S. Saikumar and N. Mandava, "Comparative analysis of earth quake resistant building design by considering bracings and shear wall system in ETABS software," *Mater. Today Proc.*, vol. 52, pp. 1831–1840, 2022, doi: 10.1016/j.matpr.2021.11.490.

[16] A. Haque, A. Masum, M. Ratul, and Z. Tafheem, "(PDF) EFFECT OF DIFFERENT BRACING SYSTEMS ON THE STRUCTURAL PERFORMANCE OF STEEL BUILDING," in *ResearchGate*, Sep. 2025. Accessed: Sep. 26, 2025. [Online]. Available: https://www.researchgate.net/publication/327100656_EFFECT_OF_DIFFERENT_BRACING_SYSTEMS_ON_THE_STRUCTURAL_PERFORMANCE_OF_STEEL_BUILDING

[17] H. K.M and S. G.V, "Stability analysis of rigid steel frames with and without bracing systems under the effect of seismic and wind loads," *Int. J. Civ. Struct. Eng. Res.*, vol. 2, no. 1, pp. 137–142, Apr. 2014.